6576–6591 *Nucleic Acids Research, 2018, Vol. 46, No. 13* *Published online 31 May 2018*
doi: 10.1093/nar/gky449

Methylation of hypoxia-inducible factor (HIF)-1α by G9a/GLP inhibits HIF-1 transcriptional activity and cell migration

Lei Bao[1], Yan Chen[1], Hsien-Tsung Lai[2], Shwu-Yuan Wu[2,3], Jennifer E. Wang[1], Kimmo J. Hatanpaa[1], Jack M. Raisanen[1], Miles Fontenot[4], Bradley Lega[5], Cheng-Ming Chiang[2,3,6], Gregg L. Semenza[7], Yingfei Wang[1,8,*] and Weibo Luo[1,6,*]

[1]Department of Pathology, UT Southwestern Medical Center, Dallas, TX 75390, USA, [2]Simmons Comprehensive Cancer Center, UT Southwestern Medical Center, Dallas, TX 75390, USA, [3]Department of Biochemistry, UT Southwestern Medical Center, Dallas, TX 75390, USA, [4]Medical Scientist Training Program, UT Southwestern Medical Center, Dallas, TX 75390, USA, [5]Department of Neurological Surgery, UT Southwestern Medical Center, Dallas, TX 75390, USA, [6]Department of Pharmacology, UT Southwestern Medical Center, Dallas, TX 75390, USA, [7]Vascular Program, The Johns Hopkins Institute for Cell Engineering, Baltimore, MD 21205, USA and [8]Department of Neurology and Neurotherapeutics, UT Southwestern Medical Center, Dallas, TX 75390, USA

Received October 03, 2017; Revised April 16, 2018; Editorial Decision May 08, 2018; Accepted May 09, 2018

ABSTRACT

Hypoxia-inducible factor 1 (HIF-1) is a master transcriptional regulator in response to hypoxia and its transcriptional activity is crucial for cancer cell mobility. Here we present evidence for a novel epigenetic mechanism that regulates HIF-1 transcriptional activity and HIF-1-dependent migration of glioblastoma cells. The lysine methyltransferases G9a and GLP directly bound to the α subunit of HIF-1 (HIF-1α) and catalyzed mono- and di-methylation of HIF-1α at lysine (K) 674 *in vitro* and *in vivo*. K674 methylation suppressed HIF-1 transcriptional activity and expression of its downstream target genes *PTGS1*, *NDNF*, *SLC6A3*, and *Linc01132* in human glioblastoma U251MG cells. Inhibition of HIF-1 by K674 methylation is due to reduced HIF-1α transactivation domain function but not increased HIF-1α protein degradation or impaired binding of HIF-1 to hypoxia response elements. K674 methylation significantly decreased HIF-1-dependent migration of U251MG cells under hypoxia. Importantly, we found that G9a was downregulated by hypoxia in glioblastoma, which was inversely correlated with *PTGS1* expression and survival of patients with glioblastoma. Therefore, our findings uncover a hypoxia-induced negative feedback mechanism that maintains high activity of HIF-1 and cell mobility in human glioblastoma.

INTRODUCTION

Hypoxia-inducible factor 1 (HIF-1), consisting of an O_2-regulated HIF-1α subunit and a constitutively expressed HIF-1β subunit, is a master regulator of transcriptional responses to reduced oxygen availability in metazoans (1). HIF-1 transactivates hundreds of downstream target genes, whose protein products control many aspects of cancer biology, including angiogenesis, metabolism, pH homeostasis, stem cell pluripotency, immune evasion and cell migration/invasion (2). Thus, the transcriptional activity of HIF-1 is crucial for cancer development.

HIF-1α protein is heavily conjugated with multiple post-translational modifications, which play a key role in modulating HIF-1 transcriptional activity. Ubiquitination represents the best-studied mechanism of indirect regulation of HIF-1 transcriptional activity (3,4). In well-oxygenated cells, HIF-1α is hydroxylated on proline 402 and 564 by prolyl hydroxylases (5–7). Hydroxylated proline residues are the docking sites for the von Hippel-Lindau (VHL)/Cullin-2/Elongin-B/C ubiquitin E3 ligase complex, which mediates HIF-1α ubiquitination and subsequent proteasomal degradation (7,8). Our previous studies showed that HIF-1α ubiquitination by the ubiquitin E3 ligase CHIP mediates VHL-independent HIF-1α protein decay and inhibition of HIF-1 transcriptional activity under prolonged hypoxia (9). Other post-translational modifications, such as acetylation and phosphorylation, influence the HIF-1α ubiquitination pathway to alter HIF-1α protein stability and activation (10,11). HIF-1α is acetylated at lysine (K) 674 by an acetyltransferase p300/CBP-associated factor (PCAF),

*To whom correspondence should be addressed. Tel: +1 214 645 4770; Fax: +1 214 648 1102; Email: Weibo.Luo@UTSouthwestern.edu
Correspondence may also be addressed to: Yingfei Wang. Tel: +1 214 645 7961; Fax: +1 214 648 1102; Email: Yingfei.Wang@UTSouthwestern.edu

and deacetylated by a deacetylase Sirtuin 1 (12). Sirtuin 2 was also shown to deacetylate K709 of HIF-1α to increase HIF-1α ubiquitination and degradation, thereby inhibiting HIF-1 transcriptional activity (13). Recent studies have identified monomethylation (me1) of K32 and dimethylation (me2) of K391 of HIF-1α by SET7/9, which is counteracted by lysine-specific demethylase 1 (LSD1) (14–16). Although SET7/9 decreases HIF-1 transcriptional activity, its underlying mechanism is still under debate (14,15). Nevertheless, most studies have paid attention to the role of post-translational modifications in HIF-1α protein stability. Yet it remains poorly understood whether lysine methylation occurs at the transactivation domain of HIF-1α to directly modulate HIF-1 transcriptional activity in cancer cells.

The lysine methyltransferase G9a is a member of the Suv39h family and mediates gene silencing by inducing methylation of K9 on histone H3 (H3K9) (17). A vast array of genes is repressed by G9a, leading to effects on proliferation, autophagy, epithelial–mesenchymal transition, and cancer development (18–20). Apart from methylating histones, G9a also methylates non-histone proteins, including p53, WIZ, CDYL1, ACINUS, Reptin, Pontin and itself (21–23). G9a-methylated Pontin and Reptin exert distinct functions on HIF-1 activity (22,23). Methylated Pontin stimulates HIF-1 transcriptional activity through increasing p300 recruitment in breast cancer cells, whereas Reptin methylation suppresses HIF-1 transcriptional activity (22,23). A recent study found that G9a protein is stabilized by hypoxia and mediates hypoxia-induced transcriptional repression in breast cancer cells (24). However, the precise role of G9a in HIF-1 transcriptional activity remains unclear.

In the present study, we found that G9a and its paralog G9a-like protein (GLP) interact with HIF-1α and directly catalyze K674me1/2 of HIF-1α *in vitro* and in human cells. G9a/GLP-mediated K674 methylation decreases HIF-1 transcriptional activity and expression of a subset of HIF-1 downstream target genes in glioblastoma multiforme (GBM) cells, leading to inhibition of GBM cell migration. G9a is downregulated in GBM cells subjected to chronic hypoxia and in human GBM tissues, and its expression is negatively correlated with HIF-1 target gene expression as well as the clinical outcome in patients with GBM. Together, these findings uncover a novel negative feedback mechanism of HIF-1 transcriptional activity in GBM.

MATERIALS AND METHODS

Plasmid constructs

Human full-length G9a and its catalytically dead mutant (H1113K) cDNAs were amplified by PCR from FLAG-G9a and FLAG-G9a (H1113K) plasmids, respectively, and subcloned into pcDNA3.1-V5-His vector (Invitrogen) or lentiviral cFugw-FLAG vector. Human HIF-1α subdomain cDNAs were amplified by PCR from FLAG-HIF-1α plasmid and subcloned into pGex-6P-1 (GE Healthcare). Full-length HIF-1α cDNA was subcloned into lentiviral cFugw-FLAG vector. HIF-1α mutants (K625R, K629R, K636R, K649R, K674R and K674Q) were generated by site-directed mutagenesis PCR. Human HIF-1α, HIF-2α, G9a and GLP sgRNAs were designed by the online CRISPR design program (http://crispr.mit.edu), annealed and cloned into lentiCRISPRv2 vector (Addgene #52961). The sgRNA oligonucleotide sequences are listed in Supplementary Table S1. pSG5-GLP-HA was a gift from Xiaodong Cheng (UT MD Anderson Cancer Center). Other plasmids were described previously (25,26). All plasmids were confirmed by DNA sequencing.

Cell culture, transfection and hypoxia

HeLa, HEK293FT, LN-229, U87MG and U251MG cells were cultured in high glucose DMEM (Sigma) supplemented with heat-inactivated 10% fetal bovine serum (FBS, Sigma) at 37°C in a 5% CO_2/95% air incubator. All cell lines are mycoplasma-free and have been authenticated by STR DNA profiling analysis. Cells were transfected using PolyJet (SignaGen) or FuGENE 6 (Promega) according to the manufacturer's instruction. CRISPR/Cas9 knockout (KO) cells were generated by transfection of U251MG or HeLa cells with sgRNA vector and subsequent treatment with puromycin. A single KO cell was selected and verified by genotyping and immunoblot assays. For hypoxia, cells were placed at 37°C in a modular chamber (Billups-Rothenberg), which was flushed with a gas mixture containing 1% O_2, 5% CO_2, and balanced N_2.

Lentivirus production

The lentivirus was generated by transfection of HEK293FT cells with transducing vector and packaging vectors psPAX2 (Addgene #12260) and pMD2.G (Addgene #12259). Forty eight hours after transfection, the supernatant containing virus particles was collected, filtered and transduced into U251MG cells.

Immunoprecipitation (IP) and immunoblot assays

Cells were lysed in lysis buffer [10 mM Tris–HCl (pH 8.0), 150 mM NaCl, 1 mM EDTA, 0.5% NP-40 and protease inhibitor cocktail] for 30 min on ice, followed by centrifugation at 13 000 *g* for 15 min at 4°C. Whole-cell lysates (WCLs) were subjected to IP by incubation overnight at 4°C with a primary antibody in the presence of protein G magnetic beads (Bio-Rad). After extensive washing with lysis buffer, the bound proteins were eluted by boiling in SDS-PAGE sample buffer, and analyzed by immunoblot assays. Antibodies used for IP and immunoblot assays are the following: anti-methyl lysine (ab23366, Abcam; NB600-824, Novus Biologicals); anti-HIF-1α (sc-10790, Santa Cruz; 610959, BD Biosciences); anti-HIF-2α (A300-286A, Bethyl Laboratories); anti-G9a (G6919, Sigma); anti-GLP (A301-642A, Bethyl Laboratories); p300 (NB500-161, Novus Biologicals); anti-JMJD2C (NBP1-49600, Novus Biologicals); anti-Pontin (12300S, Cell Signaling Technology); anti-Reptin (8959S, Cell Signaling Technology); anti-FLAG (F3165, Sigma); anti-V5 (R96025, Invitrogen); anti-HA (H9658, Sigma); anti-monomethyl and anti-dimethyl HIF-1α K674 antibodies (Novus Biologicals).

In vitro methylation assays

The methyltransferases G9a [210–1210 amino acid (aa)], GLP (32–1298 aa), SET7, SMYD2, and SET8 were expressed in Sf9 cells and purified as described previously (26). GST-HIF-1α proteins were expressed in *Escherichia coli* BL21-Gold (DE3) and purified by binding to glutathione–Sepharose beads (GE Healthcare) (25). Purified methyltransferases (200 ng) were incubated at 30°C for 1 h with a GST-HIF-1α protein in methylation reaction buffer [40 mM Tris–HCl (pH 8.5), 100 mM NaCl, 30 mM KCl, 6% glycerol and 55 μCi/ml *S*-Adenosyl-L-(methyl-^{3}H)methionine (^{3}H-SAM) or 100 μM unlabeled SAM (PerkinElmer)]. The reaction was terminated by adding SDS-PAGE sample buffer and boiling for 2 min. HIF-1α methylation was determined by autoradiography, mass spectrometry, or immunoblot assays with anti-monomethyl or dimethyl HIF-1α K674 antibodies.

Mass spectrometry (MS) assays

Purified GST-HIF-1α (576–680 aa) protein was incubated with purified G9a (210–1210) in *in vitro* methylation assays, fractionated by SDS-PAGE, and stained by Coomassie blue. Stained GST-HIF-1α (576–680) protein was excised, reduced with DTT (Sigma), alkylated with iodoacetamide (Sigma), and digested with endoproteinase Arg-C (Sigma). Following solid-phase extraction cleanup with Oasis HLB plates (Waters), the resulting peptides were injected and analyzed by LC/MS/MS using a Q Exactive HF mass spectrometer (Thermo) coupled to an Ultimate 3000 RSLC-Nano liquid chromatography system (Dionex). Samples were separated on a 75-μm i.d., 50-cm Easy Spray column (Thermo) and eluted with a gradient from 1–28% buffer B (80% (v/v) acetonitrile, 10% (v/v) trifluoroethanol and 0.08% formic acid) over 60 min at a 400 nl/min flow rate. The mass spectrometer was operated in positive ion mode with a source voltage of 2.2 kV, capillary temperature of 275°C, and S-lens RF level at 55%. MS scans were acquired at 120,000 resolution and up to 20 MS/MS spectra were obtained for each full spectrum acquired using higher-energy collisionally-induced dissociation (HCD) for ions with charge 2–8. Raw MS data files were converted to a peak list format and analyzed using the central proteomics facilities pipeline (version 2.0.3). Peptide identification was performed using the Tandem and open MS search algorithm search engines against the human protein database from Uniprot, with common contaminants and reversed decoy sequences appended. Fragment and precursor tolerances of 20 ppm and 0.5 Da were specified, and three missed cleavages were allowed. Carbamidomethylation of cysteine was set as a fixed modification, with oxidation of methionine and mono-, di- and tri-methylation of lysine as variable modifications. An additional requirement of two unique peptide sequences per protein was used for protein identification. Methylated peptides were manually verified.

Luciferase reporter assays

Parental or HIF-1α KO HeLa cells were seeded onto a 48-well plate, and transfected with HIF-1 luciferase reporter p2.1 plasmid, or pG5E1bLuc and pGalA reporter plasmid; control reporter pSV-Renilla plasmid; and expression vector encoding wild-type (WT) or catalytically dead mutant (H1113K) G9a, GLP, WT or K674R FLAG-HIF-1α, or empty vector (EV). Eighteen hours after transfection, cells were exposed to 20% or 1% O_2 for 24 hours. The firefly and Renilla luciferase activities were measured by the Dual-Luciferase Assay System (Promega).

Quantitative reverse transcription-polymerase chain reaction (RT-qPCR) assays

Total RNA was isolated with Trizol (Invitrogen) and treated with DNase I (Ambion). 1 μg of DNA-free total RNA was reverse transcribed using iScript reverse transcription kit (Bio-Rad), and resulting cDNAs were diluted and analyzed by real-time qPCR with iTaq Universal SYBR Green Supermix (Bio-Rad). Primer sequences are listed in Supplementary Table S2. The target mRNA transcript levels were normalized into 18*S* rRNA and its fold change by hypoxia was calculated based on the threshold cycle (Ct) as $2^{-\Delta(\Delta Ct)}$, where $\Delta Ct = Ct_{target} - Ct_{18S\ rRNA}$ and $\Delta(\Delta Ct) = \Delta Ct_{1\%\ O2} - \Delta Ct_{20\%\ O2}$ (25).

Chromatin immunoprecipitation (ChIP)-qPCR assays

Cells were crosslinked with 1% formaldehyde for 20 min, and quenched in 0.125 M glycine. After washing with PBS plus protease inhibitor cocktail, cells were lysed in lysis buffer (50 mM Tris–HCl, 10 mM EDTA, 1% SDS, and protease inhibitor cocktail). The chromatin was fragmented by sonication, diluted in ChIP IP buffer [0.01% SDS, 1% Triton X-100, 2 mM EDTA, 20 mM Tris–HCl (pH 8.1), 150 mM NaCl, and protease inhibitor cocktail], and subjected to IP by incubation overnight at 4°C in the presence of protein A agarose beads pre-blocked with salmon sperm DNA (Millipore) with following antibodies: G9a (G6919, Sigma); GLP (A301–642A, Bethyl Laboratories); p300 (NB500-161, Novus Biologicals); H3K9me2 (4658S, Cell Signaling Technology); rabbit IgG (2729S, Cell Signaling Technology). For FLAG ChIP, a SimpleChIP Kit (#9003, Cell Signaling Technology) was used for preparation of chromatin according to manufacturer's protocol. Briefly, cells were resuspended in buffer A on ice for 10 min. After centrifugation, cells were resuspended in buffer B and digested with micrococal nuclease for 20 min at 37°C, followed by termination of enzyme digestion with 0.5 M EDTA. The nuclear pellets were then collected by centrifugation, resuspended in 1× ChIP buffer containing protease inhibitor cocktail, and sonicated. The fragmented chromatin was subjected to IP in the presence of Salmon sperm DNA/protein A beads with antibodies against FLAG (F1804, Sigma) or mouse IgG (sc-2025, Santa Cruz Biotechnology) overnight at 4°C. The precipitated chromatin DNA was washed, eluted, reverse crosslinked at 65°C for 4 h followed by treatment with proteinase K at 45°C for 1 h, purified with phenol/chloroform/isoamyl alcohol (25:24:1, v/v), and quantified by real-time qPCR assays. The primers used for ChIP-qPCR are listed in Supplementary Table S2. Fold enrichment was calculated based on Ct as $2^{-\Delta(\Delta Ct)}$, where $\Delta Ct = Ct_{IP} - Ct_{Input}$ and $\Delta(\Delta Ct) = \Delta Ct_{antibody} - \Delta Ct_{IgG}$.

Cell migration assays

Cells were suspended in serum-free DMEM and seeded onto Boyden chamber transwell inserts (Corning). DMEM with 10% FBS was placed at the bottom plate as chemoattractant. After exposure to 20% or 1% O_2 for 16 h, cells that migrated to the lower side of the transwell insert were fixed in methanol, stained with 0.5% crystal violet, and counted.

Human GBM tissues

The study was approved by the Institutional Review Board at UT Southwestern Medical Center with informed consent. The pathology of GBM tissues were confirmed by two experienced pathologists (Kimmo J. Hatanpaa and Jack M. Raisanen). The brain tissues adjacent to GBM (<10% of tumor cells) or from patients with epilepsy were used as normal control.

Statistical analysis

All experiments were repeated at least three times. Data were expressed as mean ± SEM. Statistical analysis was performed by Student's *t*-test between two groups, or one-way or two-way ANOVA between multiple groups using GraphPad Prism7 software. Gene expression correlation was analyzed by Pearson correlation coefficients. Kaplan–Meier survival curve was analyzed by log-rank test. $P < 0.05$ is considered significant.

RESULTS

Identification of HIF-1α as a new G9a substrate

To determine if the transactivation domain of HIF-1α is lysine-methylated under hypoxia, HeLa cells were transfected with FLAG-HIF-1α (531–826) vector and exposed to 1% O_2 for 24 h. Using a pan methyl-lysine antibody (anti-Lys-me), which recognizes mono-, di- and tri-methyl lysine, we found that anti-Lys-me antibody, but not control IgG, precipitated FLAG-HIF-1α (531–826) (Figure 1A). Full-length FLAG-HIF-1α was also precipitated by anti-Lys-me antibody in HeLa cells exposed to 1% O_2 for 24 h (Figure 1B). These data indicate that HIF-1α is methylated on lysine within its transactivation domain in hypoxic human cells.

To identify which methyltransferase methylates HIF-1α, we performed a small-scale *in vitro* methylation screen. G9a, SET7, SET8 and SMYD2, which are known methyltransferases for non-histone proteins, were chosen for this screen. GST-HIF-1α (531–826) was expressed in bacteria, purified, and incubated with G9a (210–1210), SET7, SET8 or SMYD2, which were expressed and purified from insect Sf9 cells (26), in the presence of a methyl donor ^{3}H-SAM. Transfer of the ^{3}H-labeled methyl group to GST-HIF-1α (531–826) by a methyltransferase was detected by autoradiography. As shown in Figure 1C, GST-HIF-1α (531–826) was methylated by G9a (210–1210) in a concentration-dependent manner. However, no ^{3}H-SAM-labeled GST-HIF-1α (531–826) was detected when GST-HIF-1α (531–826) was incubated with SET7, SET8, SMYD2 or buffer alone (Figure 1C). These data indicate that G9a, but not SET7, SET8 or SMYD2, methylates the transactivation domain of HIF-1α *in vitro*.

To determine whether the catalytic activity of G9a is required for HIF-1α methylation, we incubated GST-HIF-1α (531–826) with WT or catalytically inactive (H1113K) G9a (210–1210) in the *in vitro* ^{3}H-SAM-based methylation assays. WT G9a (210–1210) induced methylation of GST-HIF-1α (531–826) (Figure 1D), which validated the screen data (Figure 1C). In contrast, a catalytically inactive G9a mutant (H1113K) failed to methylate GST-HIF-1α (531–826) (Figure 1D). These data indicate that G9a directly methylates HIF-1α through its methyltransferase activity *in vitro*.

To determine whether G9a methylates HIF-1α *in vivo* and whether G9a-mediated HIF-1α methylation is regulated by O_2, we employed a mutant HIF-1α (P402/564A), which is not subjected to O_2-dependent protein degradation (6), and compared the methylation levels of HIF-1α (P402/564A) that is equally expressed under normoxic and hypoxic conditions. HeLa cells were co-transfected with vector encoding FLAG-tagged HIF-1α (P402/564A), and WT or H1113K G9a or EV, and exposed to 20% or 1% O_2 for 24 h. Consistent with *in vitro* findings (Figure 1D), WT but not H1113K G9a induced methylation of FLAG-HIF-1α (P402/564A) in HeLa cells, and its methylation levels were comparable under 20% and 1% O_2 conditions (Figure 1E). These data indicate that G9a methylates HIF-1α through its methyltransferase activity in a O_2-independent manner *in vivo*.

G9a methylates HIF-1α at K674 *in vitro* and *in vivo*

To systematically map HIF-1α domains methylated by G9a, we performed *in vitro* ^{3}H-SAM-based methylation assays using a series of truncated GST-HIF-1α proteins. As expected, G9a (210–1210) methylated GST-HIF-1α (531–826) (Figure 2A). In contrast, G9a (210–1210) failed to methylate GST-HIF-1α (1–80), (81–200), (201–329), (331–427) and (432–528), or GST (Figure 2A). SET7 was known to methylate HIF-1α at lysine 32 (14). Our *in vitro* methylation assay also showed that GST-HIF-1α (1–80) was methylated by SET7 (Figure 2A), validating our experimental system. Together, these data indicate that G9a exclusively methylates HIF-1α (531–826), but not other HIF-1α domains.

To identify the lysine residue of HIF-1α methylated by G9a, we first divided HIF-1α (531–826) into 6 subdomains. *In vitro* ^{3}H-SAM-based methylation assays showed that G9a (210–1210) strongly methylated GST-HIF-1α (576–680) and (576–786), comparable to its effect on GST-HIF-1α (531–826) methylation (Figure 2B). In contrast, GST-HIF-1α (531–575), (681–786) and (787–826) were not methylated by G9a (210–1210) (Figure 2B). These data indicate that G9a-methylated lysine residue resides within the amino acid residues 576–680 of HIF-1α. The HIF-1α (576–680) subdomain contains a total of five lysine residues. Mutation of K674 to arginine (K674R) in this subdomain completely abolished G9a (210–1210)-induced GST-HIF-1α (531–826) methylation *in vitro* (Figure 2C). In contrast, individual mutation of the other four lysine residues did not alter G9a (210–1210)-induced GST-HIF-1α (531–826) methylation (Figure 2C).

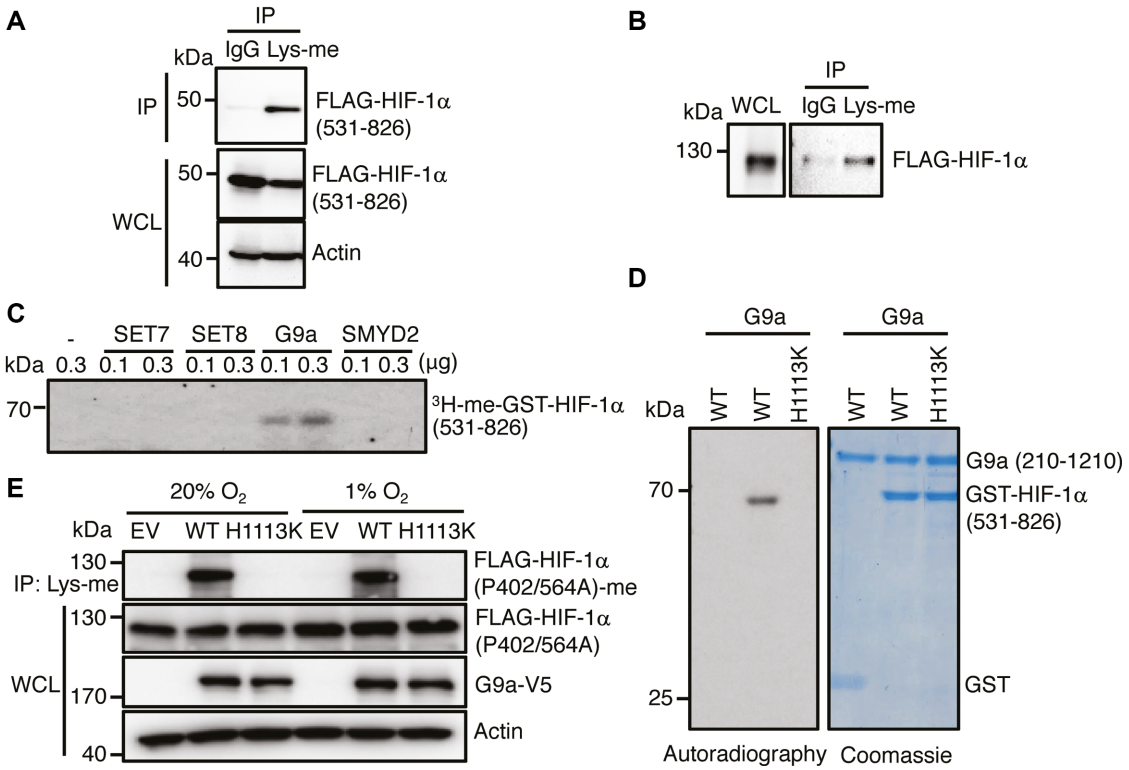

Figure 1. HIF-1α is methylated by G9a. (**A** and **B**) HeLa cells were transfected with FLAG-HIF-1α (531–826) (A) or FLAG-HIF-1α (B) vector and exposed to 1% O_2 for 6 h. IP assays were performed with IgG or anti-Lys-me antibody, followed by immunoblot assays with antibodies against FLAG or actin. (**C** and **D**) *In vitro* methylation assays were performed using purified GST-HIF-1α (531–826) and methyltransferases in the presence of ^{3}H-SAM, followed by autoradiography or Coomassie staining. (**E**) HeLa cells were cotransfected with FLAG-HIF-1α (P402/564A) vector and WT or inactive H1113K G9a or EV, and exposed to 20% or 1% O_2 for 24 h. IP assays were performed with anti-Lys-me antibody, followed by immunoblot assays with antibodies against FLAG or V5.

To confirm K674 methylation and to identify its methylation type by G9a, we performed MS assays. GST-HIF-1α (576–680) was incubated with G9a (210–1210) in the presence of SAM, fractionated by SDS-PAGE, and subjected to MS analysis. Two major methylation types K674me1 and K674me2 were identified by MS (Figure 2D–F). The percentage of the K674me1- and K674me2-containing peptides was 18.8% and 10.6%, respectively (Figure 2D). In contrast, few trimethyl (me3) K674-containing peptides (2.4%) were detected, similar to unmethylated K649 (Figure 2D).

To further validate the MS data, we developed polyclonal antibodies that specifically recognize K674me1 or K674me2 of HIF-1α. *In vitro* methylation assays showed that GST-HIF-1α (531–826) was indeed mono- and di-methylated at K674 in the presence of G9a (Figure 2G). K674R, but not K625R, K629R, K636R or K649R, completely abolished mono- and di-methylation of GST-HIF-1α (531–826) (Figure 2G).

We further examined if G9a methylates K674me1 and K674me2 of HIF-1α *in vivo*. IP assays showed that WT but not H1113K G9a induced K674me1 and K674me2 of FLAG-HIF-1α in HeLa cells exposed to 1% O_2 for 6 h (Figure 2H). Consistent with *in vitro* findings (Figure 2G), K674R, but not K649R, eliminated G9a-induced K674me1 and K674me2 of FLAG-HIF-1α in hypoxic HeLa cells (Figure 2H). Together, these *in vitro* and *in vivo* data indicate that G9a catalyzes mono- and di-methyl K674 of HIF-1α.

G9a interacts with and methylates endogenous HIF-1α *in vivo*

The HIF-1α methylation data shown above suggest that G9a interacts with HIF-1α. To test this possibility, HeLa cells were transfected with FLAG-G9a vector and exposed to 1% O_2 for 6 h. Anti-HIF-1α antibody pulled down FLAG-G9a in hypoxic HeLa cells, whereas control IgG failed to do so (Figure 3A). We also performed a reciprocal co-IP assay and found that anti-G9a antibody, but not IgG, precipitated FLAG-HIF-1α in hypoxic HeLa cells (Figure 3B). Furthermore, we found that endogenous G9a precipitated with endogenous HIF-1α, but not HIF-2α, in U251MG cells exposed to 1% O_2 for 6 h (Figure 3C). Together, these data indicate that G9a interacts with HIF-1α, but not HIF-2α, in human cells.

Next, we generated G9a KO HeLa cells by the CRISPR/Cas9 technique and performed IP assays to determine if G9a methylates endogenous HIF-1α *in vivo*. As shown in Figure 3D, anti-K674me1 antibody strongly precipitated endogenous HIF-1α in parental, but not G9a KO, HeLa cells under hypoxia, suggesting that G9a KO abolished monomethylation of HIF-1α at K674. Similarly, very little endogenous HIF-1α K674me2 was detected in G9a

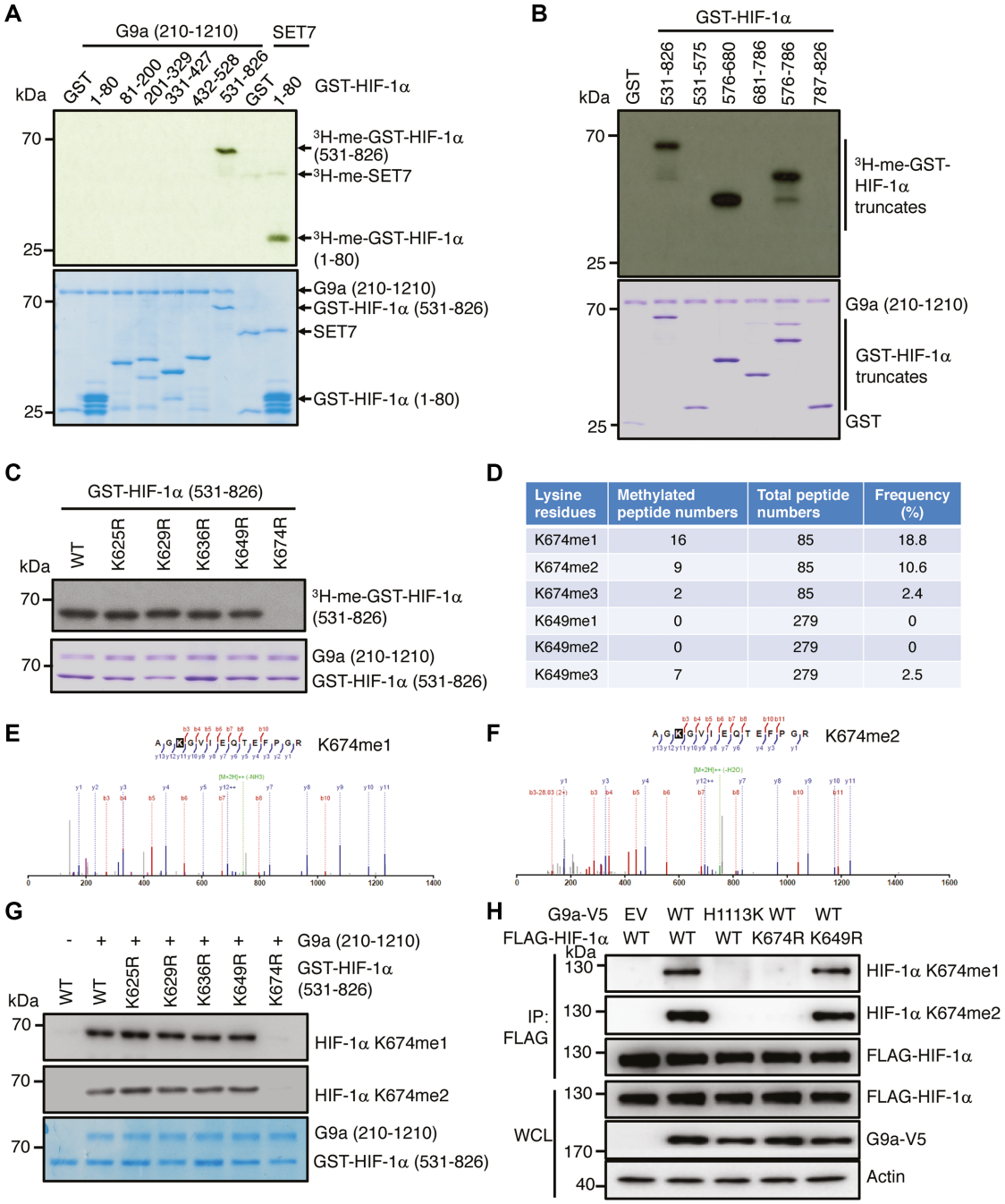

Lysine residues	Methylated peptide numbers	Total peptide numbers	Frequency (%)
K674me1	16	85	18.8
K674me2	9	85	10.6
K674me3	2	85	2.4
K649me1	0	279	0
K649me2	0	279	0
K649me3	7	279	2.5

Figure 2. G9a methylates HIF-1α at K674. (**A**–**C**) *In vitro* methylation assays were performed using GST or indicated GST-HIF-1α truncated proteins and G9a (210–1210) or SET7 in the presence of ^{3}H-SAM, followed by autoradiography or Coomassie staining. (**D**–**F**) GST-HIF-1α (576–680) was incubated with purified G9a (210–1210) in the presence of SAM, followed by MS analysis. Methylation of K674 and K649 was summarized in D. The spectra of the HIF-1α peptide containing monomethyl (E) and dimethyl (F) K674 are shown. (**G**) *In vitro* methylation assays were performed using purified WT or mutant GST-HIF-1α (531–826) and G9a (210–1210) in the presence of SAM, followed by immunoblot assays with antibodies against K674me1 or K674me2, and Coomassie staining. (**H**) HIF-1α KO HeLa cells were cotransfected with WT or mutant FLAG-HIF-1α vector and WT or catalytically inactive H1113K G9a-V5 vector or EV, and exposed to 1% O_2 for 6 h. IP assays were performed with anti-FLAG antibody, followed by immunoblot assays with antibodies against K674me1, K674me2, FLAG, V5 or actin.

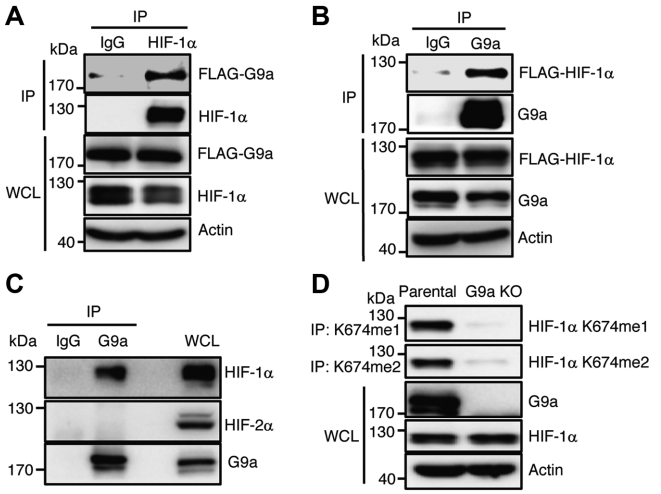

Figure 3. G9a interacts with and methylates endogenous HIF-1α. (**A**) HeLa cells were transfected with FLAG-G9a vector and exposed to 1% O_2 for 6 h. IP assays were performed with IgG or anti-HIF-1α antibody, followed by immunoblot assays with antibodies against FLAG, HIF-1α, or actin. (**B**) HeLa cells were transfected with FLAG-HIF-1α vector and exposed to 1% O_2 for 6 h. IP assays were performed with IgG or anti-G9a antibody, followed by immunoblot assays with antibodies against FLAG, G9a or actin. (**C**) U251MG cells were exposed to 1% O_2 for 6 h. IP assays were performed with IgG or anti-G9a antibody, followed by immunoblot assays with antibodies against HIF-1α, HIF-2α or G9a. (**D**) Parental or G9a KO HeLa cells were exposed to 1% O_2 for 6 h, and subjected to IP with antibodies against K674me1 or K674me2, followed by immunoblot assays with antibodies against HIF-1α, G9a or actin.

KO HeLa cells under hypoxia (Figure 3D). These data indicate that G9a catalyzes mono- and di-methylation of endogenous HIF-1α at K674 in human cells.

GLP interacts with and methylates HIF-1α

GLP often shares the same substrates with G9a (17). Thus, we studied if GLP also interacts with HIF-1α. As shown in Figure 4A, anti-GLP antibody, but not control IgG, pulled down both endogenous HIF-1α and GLP in U251MG cells under hypoxia, indicating that GLP binds to HIF-1α in human cells. Endogenous HIF-2α did not interact with GLP in hypoxic U251MG cells (Figure 4A). To determine whether GLP methylates HIF-1α, we performed *in vitro* methylation assays. Similar to G9a, GLP (32–1298) methylated GST-HIF-1α (531–826), but not GST alone *in vitro* (Figure 4B). Domain mapping studies showed that GLP (32–1298) methylated GST-HIF-1α (531–826), (576–680), and (576–786), but not GST-HIF-1α (531–575), (681–786), and (787–826), or GST (Figure 4C). K674R, but not K625R, K629R, K636R, or K649R, abolished GLP-induced mono- or di-methylation of GST-HIF-1α (531–826) *in vitro* (Figure 4D). Further, we found that ectopic expression of HA-GLP induced mono- and di-methylation of FLAG-HIF-1α in hypoxic HeLa cells (Figure 4E). Consistent with *in vitro* findings (Figure 4D), FLAG-HIF-1α (K674R) failed to be mono- and di-methylated by GLP in hypoxic HeLa cells, whereas FLAG-HIF-1α (K649R) was fully methylated by GLP like WT FLAG-HIF-1α (Figure 4E). GLP-induced HIF-1α methylation was not regulated by hypoxia (Figure 4F). Conversely, CRISPR/Cas9-based KO of GLP decreased K674me1 or K674me2 levels of endogenous HIF-1α in hypoxic HeLa cells (Figure 4G). These data indicate that GLP catalyzes mono- and di-methylation of HIF-1α at K674 *in vitro* and in human cells, as G9a does, but to a lesser extent.

G9a/GLP inhibits HIF-1 transcriptional activity and downstream target gene expression

To determine if G9a/GLP regulates HIF-1 transcriptional activity, we performed HIF-1 luciferase reporter p2.1 assays. Parental or HIF-1α KO HeLa cells were co-transfected with p2.1, containing a hypoxia response element from the *ENO1* gene upstream of the firefly luciferase gene (27), a control vector pSV-Renilla, and vector encoding WT or H1113K G9a, or EV, and exposed to 20% or 1% O_2 for 24 h. WT G9a significantly decreased HIF-1 transcriptional activity, which was reversed by catalytically inactive G9a (H1113K) in HeLa cells (Figure 5A). Neither WT nor inactive G9a altered p2.1 activity in HIF-1α KO HeLa cells (Figure 5A), indicating specific inhibition of HIF-1 by G9a. Ectopic expression of WT or H1113K G9a did not affect the protein levels of HIF-1α in HeLa cells (Figure 2H), suggesting that G9a-mediated HIF-1 inhibition is not due to reduced HIF-1α protein levels. Likewise, ectopic expression of GLP also significantly inhibited HIF-1 transcriptional activity in hypoxic HeLa cells (Figure 5B). To further determine if G9a/GLP directly inhibits HIF-1 transcriptional activity, we performed HIF-1 luciferase reporter GalA assays. HeLa cells were co-transfected with pGalA, which encodes HIF-1α (531–826) fused to the Gal4 DNA-binding domain (28), a luciferase reporter plasmid pG5E1bLuc containing five Gal4-binding sites and a TATA box upstream of the firefly luciferase gene, and WT or H1113K G9a vector, or EV, and exposed to 20% or 1% O_2 for 24 h. WT but not H1113K G9a inhibited HIF-1 transactivation in hypoxic HeLa cells (Figure 5C). Similar results were also observed in HIF-1α KO HeLa cells as GalA assays measured the activity of exogenous HIF-1α transactivation domain, not endogenous HIF-1α (Figure 5C). We also found that ectopic expression of GLP significantly decreased HIF-1 transactivation in HeLa cells (Figure 5D). Together, these data indicate that G9a/GLP inhibit HIF-1 transcriptional activity through the methyltransferase activity in hypoxic cells.

To determine whether G9a suppresses transcription of HIF-1 target genes, we generated G9a KO and G9a+HIF-1α double KO (DKO) U251MG cells by the CRISPR/Cas9 technique (Figure 5E). Parental, G9a KO, G9a+HIF-1α DKO cells were exposed to 20% or 1% O_2 for 24 h. RT-qPCR assays showed that hypoxia significantly induced transcription of HIF-1 target genes *PTGS1*, *NDNF*, *SLC6A3*, *Linc01132*, and *VEGFA* in U251MG cells (Figure 5F). Hypoxia-induced *PTGS1*, *NDNF*, *SLC6A3*, and *Linc01132* mRNA, but not *VEGFA* mRNA, was significantly enhanced in G9a KO U251MG cells as compared to parental U251MG cells (Figure 5F). As expected, HIF-1α KO abolished G9a KO-induced HIF-1 target genes (Figure 5F), suggesting that repression of these hypoxia-inducible genes is due to specific inhibition of HIF-1 by G9a. Neither HIF-1α nor HIF-2α protein levels were affected by G9a KO in nonhypoxic and hypoxic U251MG cells (Figure 5E). To

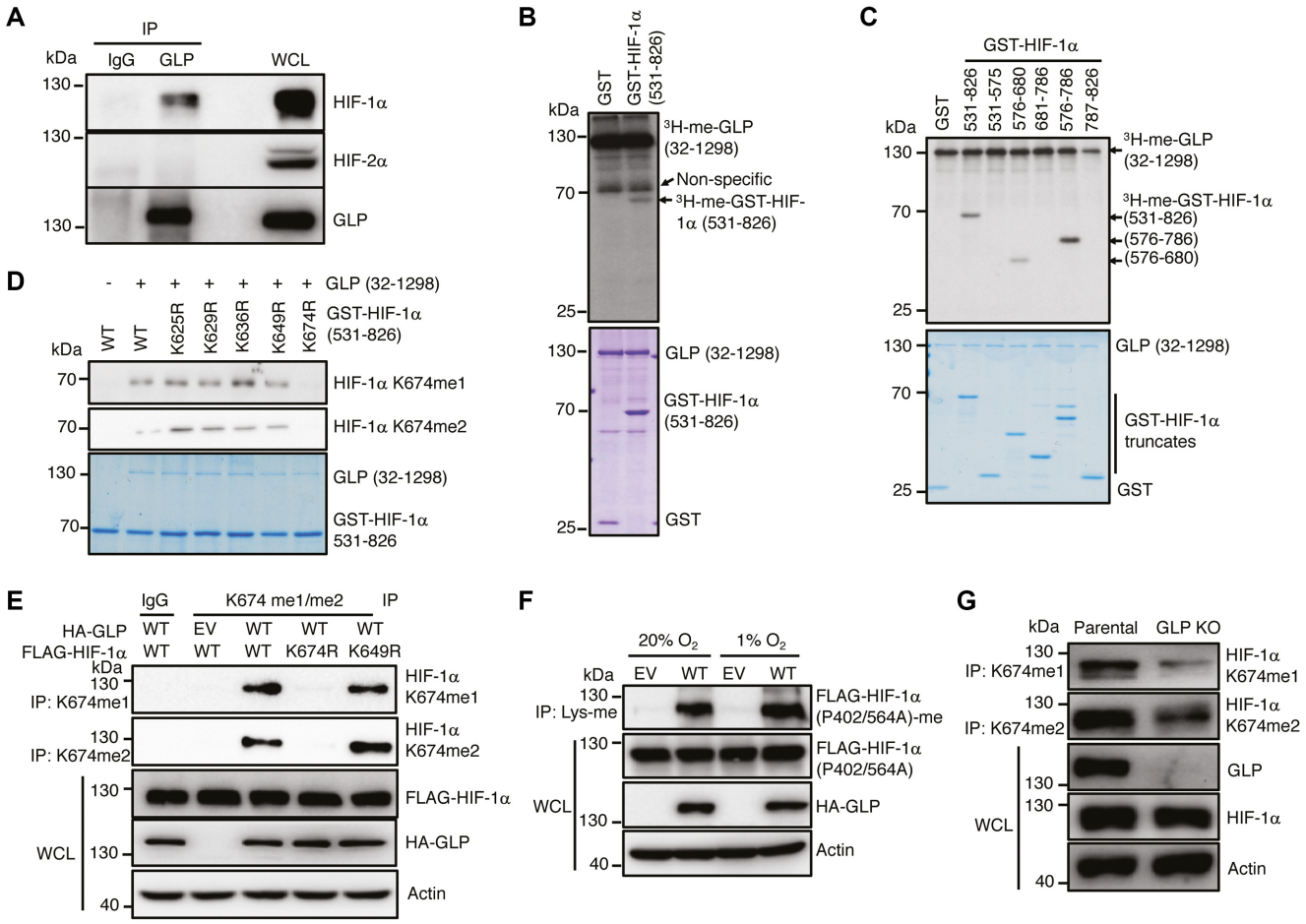

Figure 4. GLP interacts with and methylates HIF-1α at K674 *in vitro* and *in vivo*. (**A**) IP assays were performed with IgG or anti-GLP antibody in U251MG cells exposed to 1% O_2 for 6 h, followed by immunoblot assays with antibodies against GLP, HIF-1α or HIF-2α. (**B** and **C**) *In vitro* methylation assays were performed using indicated GST-HIF-1α truncated proteins or GST and GLP (32–1298) in the presence of ^{3}H-SAM, followed by autoradiography or Coomassie staining. (**D**) *In vitro* methylation assays were performed using purified WT or mutant GST-HIF-1α (531–826) and GLP (32–1298) in the presence of SAM, followed by immunoblot assays with antibodies against K674me1 or K674me2, and Coomassie staining. (**E**) HeLa cells were cotransfected with WT or mutant FLAG-HIF-1α vector and HA-GLP vector or EV, and exposed to 1% O_2 for 6 h. IP assays were performed with IgG, anti-K674me1 antibody, or anti-K674me2 antibody, followed by immunoblot assays with antibodies against FLAG, HA, or actin. (**F**) HeLa cells were cotransfected with FLAG-HIF-1α (P402/564A) vector and HA-GLP or EV, and exposed to 20% or 1% O_2 for 24 h. IP assays were performed with anti-Lys-me antibody, followed by immunoblot assays with antibodies against FLAG or HA. (**G**) Parental or GLP KO HeLa cells were exposed to 1% O_2 for 6 h, and subjected to IP with antibodies against K674me1 or K674me2, followed by immunoblot assays with antibodies against HIF-1α, GLP, or actin.

determine whether GLP has similar inhibitory functions, we generated CRISPR/Cas9-based GLP KO U251MG cells (Figure 5G). GLP KO significantly increased the expression of HIF-1 target genes *PTGS1* and *Linc01132*, but not *NDNF*, *SLC6A3*, and *VEGFA*, in U251MG cells under hypoxia (Figure 5H). These data indicate that G9a/GLP selectively inhibit HIF-1 target gene expression in U251MG cells.

K674 methylation inhibits HIF-1 transcriptional activity and target gene expression

We performed p2.1 reporter assays to determine if K674 methylation inhibits HIF-1 transcriptional activity. HeLa cells were transfected with p2.1, pSV-Renilla, and vector encoding WT or K674R FLAG-HIF-1α or EV, and exposed to 20% or 1% O_2 for 24 h. WT FLAG-HIF-1α significantly increased p2.1 activity, which was further enhanced by K674R in HeLa cells under nonhypoxic and hypoxic conditions (Figure 6A). These data indicate that K674 methylation represses HIF-1 transcriptional activity.

Next, we set out to determine whether K674 methylation suppresses the expression of HIF-1 target genes in U251MG cells. To address this, we generated HIF-1α and HIF-2α DKO U251MG cells by the CRISPR/Cas9 technique, and the rescued cell line expressing WT or K674R FLAG-HIF-1α (Figure 6B). Previous studies showed that K674 was acetylated by PCAF (12). Thus, we also generated a K674 acetylation-mimic cell line, HIF-1/2α DKO+FLAG-HIF-1α (K674Q) U251MG (Figure 6B), to distinguish the effect of K674 acetylation and methylation on HIF-1 target gene expression. These cell lines were exposed to 20% or 1% O_2 for 24 h and subjected to RT-qPCR assays. As shown in Figure 6C–G, the mRNA levels of HIF-1 target genes *PTGS1*, *NDNF*, *SLC6A3*, *Linc01132*, and *VEGFA* were increased by hy-

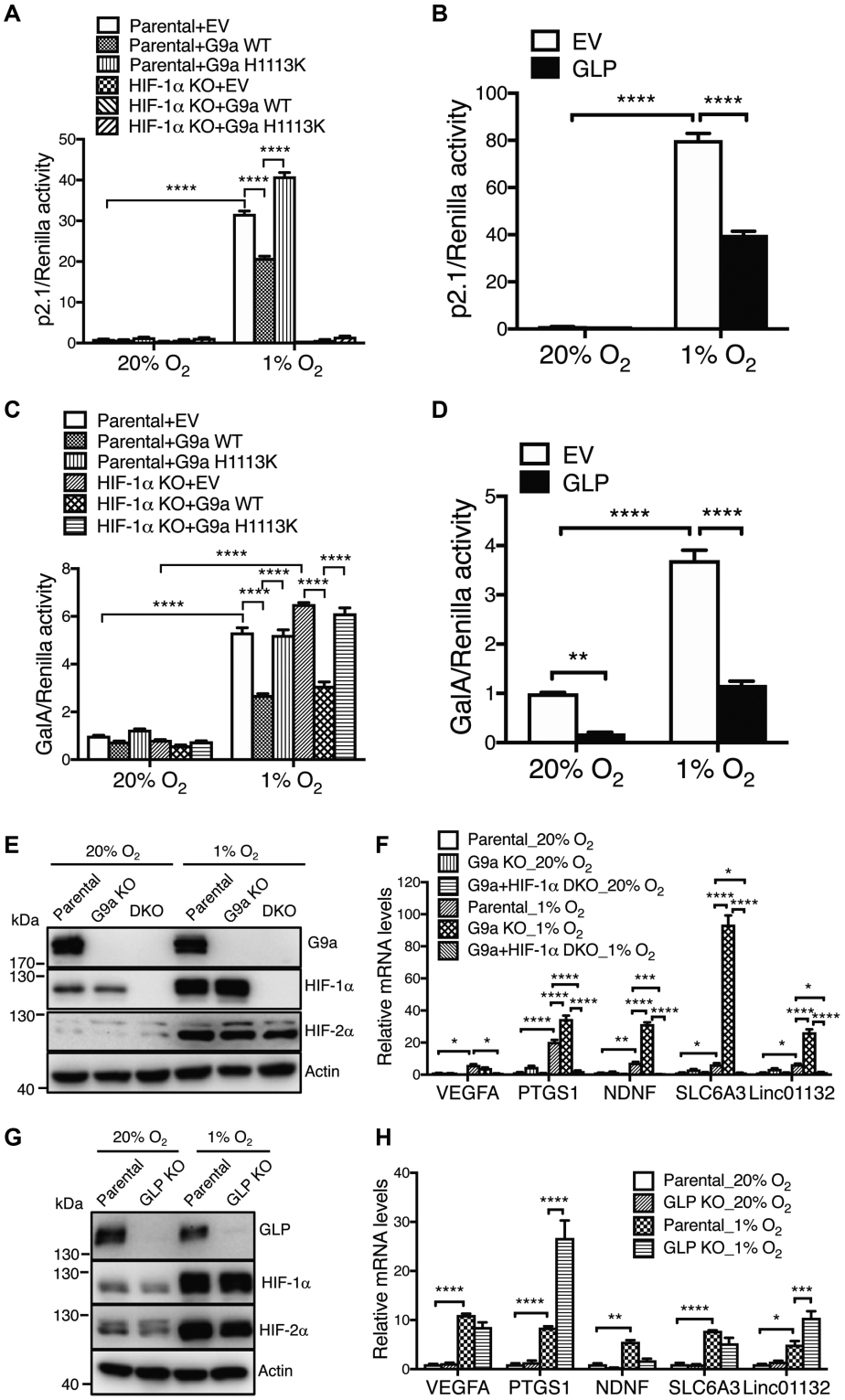

Figure 5. G9a/GLP inhibit HIF-1 transcriptional activity via their catalytic activity. (**A** and **B**) Parental or HIF-1α KO HeLa cells were cotransfected with HIF-1 luciferase reporter p2.1, pSV-Renilla and vector encoding WT G9a (A), G9a (H1113K, A), GLP (B), or EV. Cells were exposed to 20% or 1% O_2 for 24 h and subjected to dual-luciferase reporter assays ($n = 3$, mean ± SEM). $^{****}P < 0.0001$. (**C** and **D**) Parental or HIF-1α KO HeLa cells were cotransfected with pGalA, pG5E1bLuc, pSV-Renilla, and vector encoding WT G9a (C), G9a (H1113K, C), GLP (D), or EV. Cells were exposed to 20% or 1% O_2 for 24 h and subjected to dual-luciferase reporter assays ($n = 3$, mean ± SEM). $^{****}P < 0.0001$. (**E** and **F**) Parental, G9a KO, and G9a+HIF-1α DKO U251MG cells were exposed to 20% or 1% O_2 for 24 h. Immunoblot analysis of indicated proteins is shown in E. RT-qPCR analysis of indicated mRNAs is shown in F ($n = 6$, mean ± SEM). $^{*}P < 0.05$; $^{**}P < 0.01$; $^{***}P < 0.001$; $^{****}P < 0.0001$. (**G** and **H**) Parental and GLP KO U251MG cells were exposed to 20% or 1% O_2 for 24 h. Immunoblot analysis of indicated proteins is shown in G. RT-qPCR analysis of indicated mRNAs is shown in H ($n = 6$, mean ± SEM). $^{*}P < 0.05$; $^{**}P < 0.01$; $^{***}P < 0.001$; $^{****}P < 0.0001$.

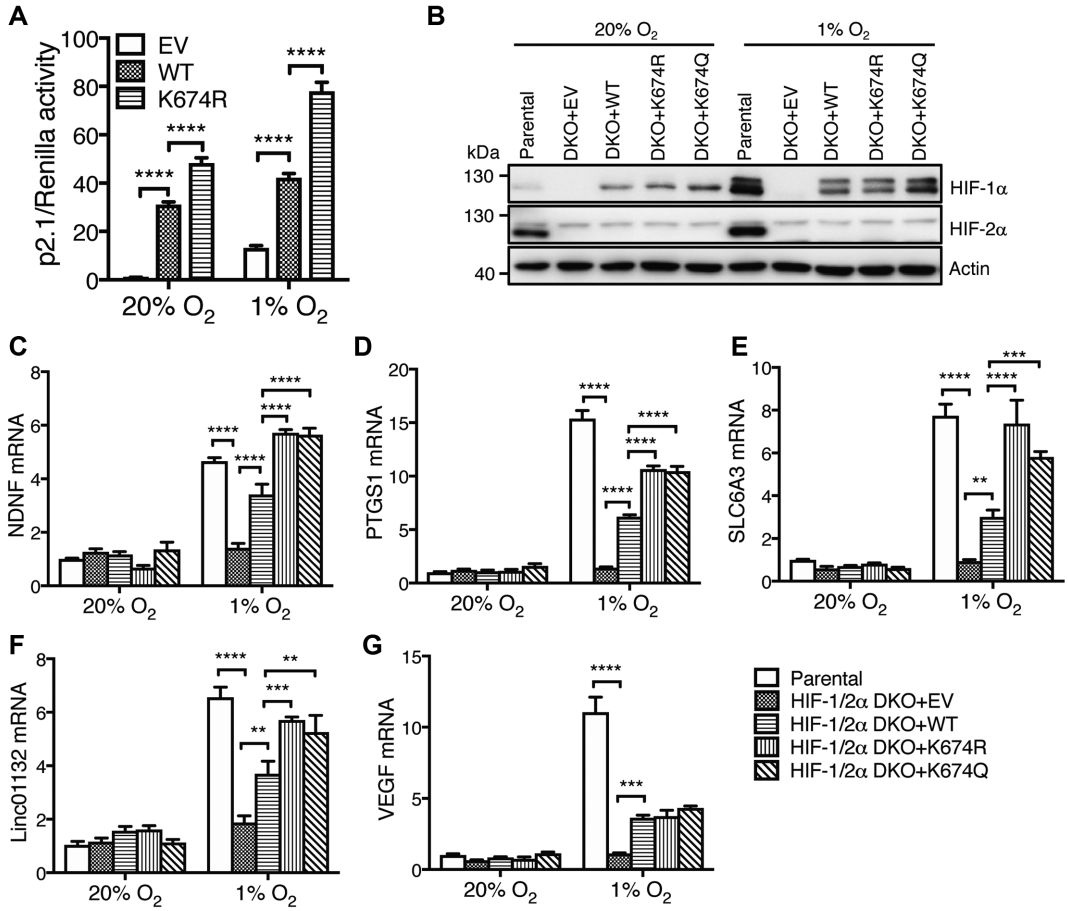

Figure 6. K674 methylation suppresses the expression of HIF-1 target genes in GBM cells. (**A**) HeLa cells were cotransfected with p2.1, pSV-Renilla, and vector encoding WT or K674R FLAG-HIF-1α, or EV. Cells were exposed to 20% or 1% O_2 for 24 h and subjected to dual-luciferase reporter assays ($n = 4$, mean ± SEM). $^{****}P < 0.0001$. (**B**–**G**) Parental, HIF-1/2α DKO+EV, HIF-1/2α DKO+WT FLAG-HIF-1α, HIF-1/2α DKO+FLAG-HIF-1α (K674R), and HIF-1/2α DKO+FLAG-HIF-1α (K674Q) U251MG cells were exposed to 20% or 1% O_2 for 24 h. Immunoblot analysis of indicated proteins is shown in B. RT-qPCR analysis of indicated mRNAs is shown in C–G ($n = 3$, mean ± SEM). $^{**}P < 0.01$; $^{***}P < 0.001$; $^{****}P < 0.0001$.

poxia, which were blocked by HIF-1/2α DKO in U251MG cells. Ectopic expression of WT FLAG-HIF-1α partially but significantly restored expression of these five HIF-1 target genes in hypoxic HIF-1/2α DKO U251MG cells (Figure 6C–G). Increased *PTGS1*, *NDNF*, *SLC6A3*, and *Linc01132* mRNA levels were significantly greater in hypoxic HIF-1/2α DKO U251MG cells expressing FLAG-HIF-1α (K674R) or (K674Q) as compared to HIF-1/2α DKO U251MG cells expressing WT FLAG-HIF-1α (Figure 6C–F), suggesting that methylation, but not acetylation, of K674 inhibits expression of *PTGS1*, *NDNF*, *SLC6A3*, and *Linc01132* in hypoxic U251MG cells. In contrast, K674R or K674Q had no effect on *VEGFA* mRNA expression in hypoxic U251MG cells (Figure 6G). The protein levels of WT, K674R, and K674Q FLAG-HIF-1α were comparable in HIF-1/2α DKO U251MG cells under hypoxia (Figure 6B), excluding the possibility that increased expression of *PTGS1*, *NDNF*, *SLC6A3*, and *Linc01132* by K674R or K674Q FLAG-HIF-1α is due to high levels of FLAG-HIF-1α (K674R) or (K674Q) protein. Therefore, these data indicate that mutation of HIF-1α at K674 phenocopies G9a loss of function by increasing HIF-1 target gene expression in U251MG cells.

K674 methylation has no effect on HIF-1 binding to the HRE

To determine whether K674 methylation inhibits HIF-1α binding to the HRE to suppress HIF-1 transcriptional activity, we performed ChIP-qPCR assays. HIF-1α KO U251MG cells were transiently transfected with vector encoding WT or K674R FLAG-HIF-1α and exposed to 20% or 1% O_2 for 24 or 72 h. As expected, WT FLAG-HIF-1α was enriched at HREs of *VEGFA*, *PTGS1*, *SLC6A3*, and *Linc01132* under non-hypoxic conditions, and its occupancy was significantly increased by hypoxia for 24 or 72 h in U251MG cells (Supplementary Figure S1A–D). Similarly, FLAG-HIF-1α (K674R) also occupied HREs of these HIF-1 target genes with binding intensity that was comparable to WT FLAG-HIF-1α (Supplementary Figure S1A–D). These data indicate that K674 methylation fails to block HIF-1 binding to HREs in GBM cells.

Chronic hypoxia reduces G9a/GLP binding to the HRE of HIF-1 target genes

Next, we studied whether G9a/GLP directly bind to the HRE of HIF-1 target genes. HIF-1α KO U251MG cells were transduced with lentivirus carrying WT or K674R

FLAG-HIF-1α and exposed to 20% or 1% O_2 for 24 or 72 h. ChIP-qPCR assays showed that G9a was highly enriched at HREs of *PTGS1*, *SLC6A3*, *Linc01132*, and *VEGFA* in HIF-1α KO U251MG cells expressing WT FLAG-HIF-1α under 20% O_2, and its enrichment was not altered by 24 h of hypoxia, but significantly decreased after 72 h of chronic hypoxia (Supplementary Figure S2A–D). Similar intensity of G9a occupancy at HREs was found in HIF-1α KO U251MG cells expressing FLAG-HIF-1α (K674R) (Supplementary Figure S2A–D). These data indicate that chronic hypoxia inhibits G9a binding to HREs, but K674 methylation has no effect on G9a enrichment at HREs. Likewise, we found that GLP also occupied HREs in U251MG cells and its occupancy was inhibited by chronic hypoxia but not K674 methylation (Supplementary Figure S2E–H). Together, these findings indicate that G9a/GLP are enriched at the HRE of HIF-1 target genes in GBM cells, and that G9a/GLP occupancy is decreased in GBM cells exposed to chronic hypoxia.

G9a/GLP are known to methylate H3K9 to suppress gene expression (17). Consistent with G9a/GLP occupancy, high enrichment of H3K9me2 was detected at HREs of *PTGS1*, *SLC6A3*, *Linc01132*, and *VEGFA* in HIF-1α KO U251MG cells expressing WT or K674R FLAG-HIF-1α under 20% O_2, and its occupancy was not increased by 24 h of hypoxia (Supplementary Figure S3A–D). These data indicate that G9a/GLP-induced H3K9 dimethylation is not responsible for repression of HIF-1 target genes in GBM cells.

p300, JMJD2C, Pontin, Reptin, PRDX2 and PRDX4 are not involved in K674 methylation-mediated HIF-1 inhibition

Next, we investigated whether K674 methylation influences the recruitment of HIF-1 coactivators or corepressors including p300, JMJD2C, Pontin, Reptin, PRDX2, or PRDX4 to HIF-1α, leading to HIF-1 inhibition. HIF-1α KO U251MG cells expressing WT or K674R FLAG-HIF-1α were exposed to 1% O_2 for 6 h. IP of p300 by anti-p300 antibody pulled down an equal amount of WT and K674R FLAG-HIF-1α (Supplementary Figure S4A), indicating that K674 methylation does not affect HIF-1α-p300 interaction in GBM cells. We further performed ChIP-qPCR assays to examine the effect of K674 methylation on the recruitment of p300 to HIF-1 target genes. Hypoxia increased p300 occupancy at HREs of *PTGS1*, *SLC6A3*, *Linc01132* and *VEGFA* in HIF-1α KO U251MG cells expressing WT FLAG-HIF-1α (Supplementary Figure S4B–E). K674R did not alter p300 occupancy under hypoxia (Supplementary Figure S4B–E). Similarly, we found that both WT and K674R FLAG-HIF-1α equally bound to JMJD2C, Pontin, Reptin, PRDX2-V5, or PRDX4-V5 in U251MG cells (Supplementary Figure S4F–I). Taken together, these findings indicate that p300, JMJD2C, Pontin, Reptin, PRDX2, and PRDX4 do not participate in K674 methylation-mediated inhibition of HIF-1 transcriptional activity in GBM cells.

HIF-1α K674 methylation impairs GBM cell migration

HIF-1 promotes cancer cell migration by inducing expression of downstream target genes (2,29). Thus, we studied if HIF-1α methylation regulates GBM cell migration by Boyden chamber migration assays. Parental, HIF-1/2α DKO+EV, HIF-1/2α DKO+WT FLAG-HIF-1α, HIF-1/2α DKO+FLAG-HIF-1α (K674R), HIF-1/2α DKO+FLAG-HIF-1α (K674Q) U251MG cells were seeded onto Boyden chamber transwell inserts, respectively, and exposed to 20% or 1% O_2 for 16 h. As expected, hypoxia significantly increased the number of cells that migrated through the transwell membrane, which was blocked by HIF-1/2α DKO (Figure 7A and B). Expression of WT FLAG-HIF-1α partially restored the migration ability of HIF-1/2α DKO U251MG cells under hypoxia (Figure 7A and B). K674R or K674Q FLAG-HIF-1α significantly increased hypoxia-induced U251MG cell migration as compared to WT FLAG-HIF-1α (Figure 7A and B). These data indicate that K674 methylation inhibits HIF-1-mediated migration of GBM cells.

G9a is downregulated by chronic hypoxia and inversely correlated with HIF-1 target gene expression in GBM

We studied if G9a/GLP proteins are regulated by hypoxia in GBM cells. U251MG cells were exposed to 20% or 1% O_2 for 24–72 h. As shown in Figure 8A, G9a protein levels were decreased in U251MG cells after 48 h of hypoxia. Hypoxia-induced G9a protein downregulation was also observed in other GBM cell lines, LN-229 and U87MG cells, in a time-dependent manner (Figure 8B and C). GLP protein was also downregulated by hypoxia in U251MG and LN229, but not U87MG cells (Figure 8A–C). In line with reduced G9a and GLP, HIF-1α K674me1/2 was attenuated by chronic hypoxia in U251MG cells (Figure 8A). Moreover, the interaction of HIF-1α with G9a was also blocked by chronic hypoxia in U251MG cells (Figure 8A). KO of HIF-1α, HIF-2α, or both had no effect on hypoxia-induced G9a or GLP downregulation in U251MG cells (Figure 8D), suggesting that hypoxia-induced downregulation of G9a and GLP is independent of HIF-1 and HIF-2.

To study if G9a/GLP downregulation occurs in human GBM, which contains extensive hypoxic regions, we analyzed mRNA levels of G9a and GLP using the data from The Cancer Genome Atlas (TCGA) (30), and found that G9a mRNA was significantly reduced in human GBM compared to normal brain tissues (Figure 8E). Similar results were also obtained from other publicly available microarray datasets (Figure 8F and G) (31,32). However, GLP mRNA expression varied in different GBM datasets (Figure 8H-J), suggesting its heterogeneity in GBM. We further found that G9a protein tended to be reduced in human GBM tissues as compared to normal brain tissues (Figure 8K and L), but GLP protein tended to be upregulated in human GBM tissues (Figure 8K and M). Notably, the HIF-1 target gene *PTGS1* was upregulated in GBM (Figure 8N–P), and its expression was negatively correlated with G9a mRNA levels (Figure 8Q). These data support our findings that G9a inhibits HIF-1 transcriptional activity and also suggest a general mechanism of augmented HIF-1 transactivation due to loss of G9a in GBM.

To determine the significance of G9a downregulation in patients with GBM, we performed the Kaplan-Meier analysis using the TCGA (30) and GSE4271 (33) datasets and the

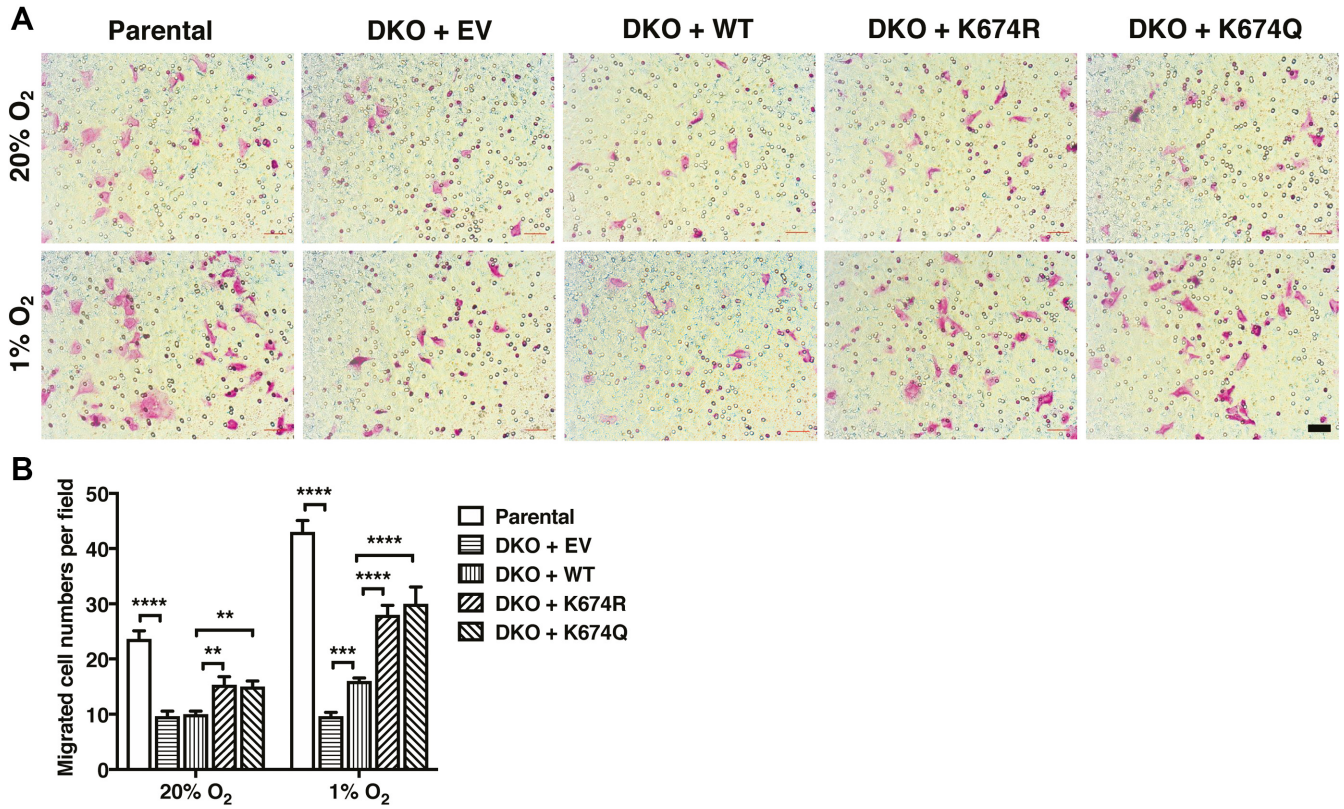

Figure 7. HIF-1α K674 methylation inhibits GBM cell migration. (**A** and **B**) Migration of parental, HIF-1/2α DKO+EV, HIF-1/2α DKO+WT FLAG-HIF-1α, HIF-1/2α DKO+FLAG-HIF-1α (K674R) and HIF-1/2α DKO+FLAG-HIF-1α (K674Q) U251MG cells in Boyden chambers under 20% or 1% O_2 for 16 h. Representative images from three experiments are shown in A. Quantification of migrated cell numbers is shown in B (mean ± SEM, $n = 3$). $^{**}P < 0.01$; $^{***}P < 0.001$; $^{****}P < 0.0001$. Scale bar, 50 μm.

PROGgene program (34), and found that low levels of G9a were significantly correlated with high mortality of GBM patients in both datasets (Figure 8R and S). No significant association between GLP mRNA levels and survival of GBM patients was observed (Figure 8T and U). These findings suggest that G9a may be a prognostic factor that predicts the clinical outcome in patients with GBM.

DISCUSSION

In the present study, we identified a novel epigenetic mechanism underlying modulation of HIF-1 transcriptional activity in GBM. The lysine methyltransferase G9a and its paralog GLP catalyzed mono- and di-methylation of HIF-1α at K674. K674 methylation directly inhibited HIF-1 transcriptional activity and downstream target gene expression in GBM cells. G9a/GLP selectively bound to HIF-1α, but not HIF-2α. Moreover, K674 was not conserved in HIF-2α, suggesting that G9a/GLP-mediated K674me1/2 are unique to HIF-1α. These data indicate HIF-1α as a new G9a/GLP substrate, and provide direct evidence that G9a/GLP inhibit HIF-1 transcriptional activity in GBM cells. Thus, G9a/GLP are the novel negative HIF-1 coregulators in GBM. G9a/GLP were enriched at the HRE of HIF-1 target genes under normoxia and their occupancy was not affected by 24 h of hypoxia, although it was impaired by chronic hypoxia possibly due to reduced G9a/GLP protein levels during chronic hypoxia. Similarly, our recent studies indicate that the HIF coactivator ZMYND8 occupies HREs and constitutes a transactivation complex under normoxic conditions, prior to HIF binding to HREs (35). These findings implicate that the HIF-1 regulatory complex containing HIF-1 coregulators has been pre-assembled at the HRE under normoxia and controls HIF-1 transcriptional activity once HIF-1 binds to the HRE under hypoxia, so that cancer cells can rapidly respond to hypoxic stress.

Although both G9a and GLP were capable to methylate HIF-1α (P402/564A) under 20% and 1% O_2, endogenous HIF-1α protein is unlikely methylated by G9a/GLP under 20% O_2 because it is unstable and degraded. We showed that both G9a and GLP bound to HREs of HIF-1 target genes under 20% O_2. Thus, G9a/GLP may methylate HIF-1α at K674 when HIF-1 occupies HREs, thereby counteracting the HIF-1-dependent transcription program. K674 methylation is impaired due to reduced G9a, GLP, and HIF-1α protein levels during chronic hypoxia. We found that G9a KO completely eliminated mono- and di-methylation of K674 of HIF-1α, whereas GLP KO partially decreased K674 methylation. These findings indicate that G9a is the primary methyltransferase for HIF-1α at K674, and that GLP methylates HIF-1α to a lesser extent. In line with their differential ability on HIF-1α methylation, G9a fully phenocopied K674 methylation-mediated inhibition of HIF-

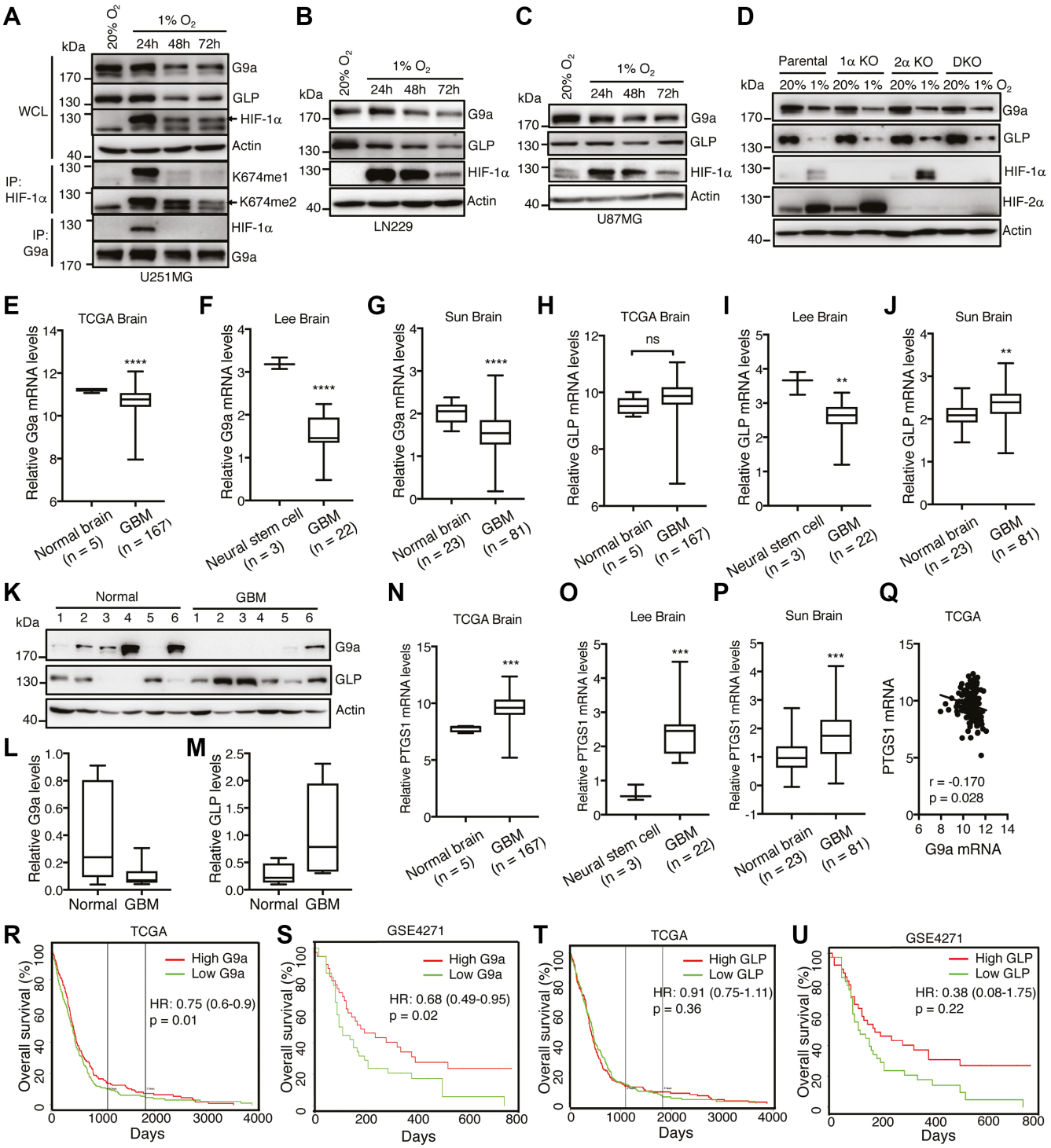

Figure 8. G9a is downregulated in GBM and anti-correlated with HIF-1 target gene expression and survival of patients with GBM. (**A–C**) U251MG (**A**), LN229 (**B**) and U87MG (**C**) cells were exposed to 20% or 1% O_2 for indicated time. IP assays were performed with anti-HIF-1α or anti-G9a antibody, followed by immunoblot assays (A). Immunoblot assays were performed with antibodies against K674me1, K674me2, G9a, GLP, HIF-1α or actin. (**D**) Parental, HIF-1α KO, HIF-2α KO or HIF-1/2α DKO U251MG cells were exposed to 20% or 1% O_2 for 48 h. Immunoblot assays were performed with antibodies against G9a, GLP, HIF-1α, HIF-2α or actin. (**E–J**) Analysis of G9a/GLP mRNA expression in normal brain and human GBM. The data were retrieved from the TCGA (E and H) (30), GSE4536 (F and I) (32), and GSE4290 (G and J) (31) databases. $^{**}P < 0.01$; $^{****}P < 0.0001$. ns, not significant. (**K–M**) Immunoblot assays were performed with antibodies against G9a, GLP, or actin in human GBM tissues and normal brain tissues (K). G9a (L) and GLP (M) bands were quantified by densitometry and normalized to actin. (**N-P**) Analysis of PTGS1 mRNA expression in normal brain and human GBM. The data were retrieved from the TCGA (**N**) (30), GSE4536 (**O**) (32), and GSE4290 (**P**) (31) databases. $^{***}P < 0.001$. (**Q**) Negative correlation between G9a and PTGS1 mRNA expression in human GBM. The data were retrieved from the TCGA (30). (**R-U**) Kaplan-Meier survival analysis for patients with GBM using the PROGgene program (34). Patients were divided by median expression levels of G9a (**R** and **S**) or GLP mRNA (**T** and **U**). HR, hazard ratio.

1 target genes *PTGS1*, *NDNF*, *SLC6A3*, and *Linc01132* in U251MG cells. GLP inhibited *PTGS1* and *Linc01132*, but not *NDNF* and *SLC6A3*. Thus, G9a may counteract the effect of GLP KO on *NDNF* and *SLC6A3* expression, whereas GLP may have little counteractive effect on HIF-1 activation by G9a loss-of-function, which is possibly due to its reduced ability to methylate HIF-1α.

Previous studies have shown that K674 is acetylated by PCAF and K674R decreases protein interaction of HIF-1α with p300 to inhibit HIF-1 transcriptional activity in HEK293T cells (12). Our data here showed that an acetylation-mimic mutant K674Q enhanced expression of the HIF-1 target genes similar to the methylation-resistant mutant K674R, suggesting that methylation but not acetylation of K674 primarily mediates repression of HIF-1 transcriptional activity in GBM cells. Recent studies identified K32me1 and K391me2 of HIF-1α by SET7/9, although it remains unclear if K391me2 is present on endogenous HIF-1α (14–16). Liu *et al.* reported that K32me1 may attenuate HIF-1 binding to the HRE of target genes (14). Subsequent studies showed that K32me1 and K391me2 decrease HIF-1α protein stability to inhibit HIF-1 transcriptional activity (15,16). In contrast to K32me1 and K391me2, K674me1/2 directly impaired HIF-1α transactivation domain activity but had no effect on HIF-1α protein stability. K674 is located in the inhibitory domain at the C-terminus of HIF-1α, which harbors the binding sites for multiple HIF-1α-interacting proteins that are involved in repression of HIF-1α transactivation domain activity (36,37). We showed that several known HIF-1 coregulators including p300, JMJD2C, Pontin, Reptin, PRDX2, and PRDX4 equally bound to unmethylated and methylated K674, and thus they are unlikely involved in G9a/GLP-mediated HIF-1 inhibition. Further studies are needed to investigate whether K674 methylation by G9a/GLP interferes with the recruitment of an unknown HIF-1 coregulator to HIF-1α leading to repression of HIF-1 transcriptional activity. We also found that K674 methylation failed to block HIF-1α binding to HREs, excluding impaired HIF-1α-DNA binding as a possible mechanism of K674 methylation-mediated HIF-1 inhibition. Nevertheless, K674 methylation represents a novel mechanism underlying inhibition of HIF-1 transcriptional activity in cancer cells.

We showed that K674 methylation suppressed expression of *PTGS1*, *NDNF*, *SLC6A3*, and *Linc01132* in U251MG cells under hypoxia, and inhibited HIF-1-dependent GBM cell migration. PTGS1 and NDNF are known to promote cell migration (38,39), suggesting an important role of PTGS1 and NDNF in K674 methylation-mediated inhibition of cell migration. Intriguingly, the HIF-1 target gene *VEGFA* was not modulated by K674 methylation. Therefore, K674 methylation selectively inhibits HIF-1-mediated transactivation of target genes in GBM cells. Selective activation or inhibition of HIF-1 target genes has been also found in many other regulatory pathways of HIF-1 activity by its coregulators (22,23,25,36,40).

Previous studies have shown that G9a is induced by hypoxia at its transcriptional levels in mouse embryonic stem cells (41). G9a protein is also stabilized through blocking its proteasomal degradation mediated by the prolyl hydroxylase/VHL pathway in MCF-7, MDA-MB-231, and A549 cells under hypoxia (24,42). However, we found that G9a was downregulated by chronic hypoxia in GBM, which was HIF-1- and HIF-2-independent. The prolyl hydroxylase/VHL pathway is functional in GBM cells as its putative substrate HIF-1α is fully regulated by this pathway in these cancer cells. Thus, cell type-specific mechanism contributes to hypoxia-mediated G9a downregulation in GBM. Notably, reduced G9a levels were correlated with increased expression of the HIF-1 target gene *PTGS1* in GBM, implying that loss of G9a-mediated HIF-1α methylation leads to high activation of HIF-1 and upregulation of HIF-1 downstream target genes in GBM. Our data suggest heterogeneous expression of GLP in GBM. To what extent GLP mediates HIF-1α methylation and HIF-1 inhibition in human GBM warrants further investigations. Together, our findings reveal a negative feedback mechanism that maintains high activity of HIF-1 in GBM.

It has been shown that G9a mediates progression of several types of human cancers, including breast cancer, liver cancer, lung cancer, and ovarian cancer (43). Targeting G9a by its small molecule inhibitors impairs tumorigenesis in mice (24). Although the precise role of G9a in GBM development remains to be determined, we showed that low levels of G9a were associated with poor survival of patients with GBM, suggesting that high activation of HIF-1 in GBM with low G9a may be the cause of high mortality of these patients and that G9a is likely a negative regulator of GBM development, distinct from its role in other cancers. HIF-1 is a key driver of GBM growth, and thus manipulating G9a-induced HIF-1α K674 methylation may benefit GBM therapy.

SUPPLEMENTARY DATA

Supplementary Data are available at NAR Online.

ACKNOWLEDGEMENTS

We thank Karen Padgett (Novus Biologicals) for providing antibodies against mono- and di-methyl K674 of HIF-1α, and Sandeep Burma (UT Southwestern) for U251MG and LN229 cell lines. We also thank UTSW Proteomics Core for mass spectrometry analysis.

FUNDING

Welch Foundation [I-1903-20160319 to W.L., I-1939-20170325 to Y.W., I-1805 to C.-M.C.]; National Institutes of Health [R00CA168746 to W.L., R00NS078049 and R35GM124693 to Y.W., CA103867 to C.-M.C.]; Susan G Komen [CCR16376227 to W.L.]; CPRIT [RR140036 to W.L., RP170671 to Y.W., RP140367 and RP180349 to C.-M.C.]. W.L. is a CPRIT Scholar in Cancer Research. Funding for open access charge: Welch Foundation.
Conflict of interest statement. None declared.

REFERENCES

1. Wang,G.L., Jiang,B.H., Rue,E.A. and Semenza,G.L. (1995) Hypoxia-inducible factor 1 is a basic-helix-loop-helix-PAS heterodimer regulated by cellular O_2 tension. *Proc. Natl. Acad. Sci. U.S.A.*, **92**, 5510–5514.

2. Semenza,G.L. (2012) Hypoxia-inducible factors: mediators of cancer progression and targets for cancer therapy. *Trends Pharmacol. Sci.*, **33**, 207–214.
3. Kallio,P.J., Wilson,W.J., O'Brien,S., Makino,Y. and Poellinger,L. (1999) Regulation of the hypoxia-inducible transcription factor 1alpha by the ubiquitin-proteasome pathway. *J. Biol. Chem.*, **274**, 6519–6525.
4. Huang,L.E., Gu,J., Schau,M. and Bunn,H.F. (1998) Regulation of hypoxia-inducible factor 1alpha is mediated by an O_2-dependent degradation domain via the ubiquitin-proteasome pathway. *Proc. Natl. Acad. Sci. U.S.A.*, **95**, 7987–7992.
5. Jaakkola,P., Mole,D.R., Tian,Y.M., Wilson,M.I., Gielbert,J., Gaskell,S.J., von Kriegsheim,A., Hebestreit,H.F., Mukherji,M., Schofield,C.J. *et al.* (2001) Targeting of HIF-alpha to the von Hippel-Lindau ubiquitylation complex by O_2-regulated prolyl hydroxylation. *Science*, **292**, 468–472.
6. Epstein,A.C., Gleadle,J.M., McNeill,L.A., Hewitson,K.S., O'Rourke,J., Mole,D.R., Mukherji,M., Metzen,E., Wilson,M.I., Dhanda,A. *et al.* (2001) C. elegans EGL-9 and mammalian homologs define a family of dioxygenases that regulate HIF by prolyl hydroxylation. *Cell*, **107**, 43–54.
7. Ivan,M., Kondo,K., Yang,H., Kim,W., Valiando,J., Ohh,M., Salic,A., Asara,J.M., Lane,W.S. and Kaelin,W.G. Jr (2001) HIFα targeted for VHL-mediated destruction by proline hydroxylation: implications for O_2 sensing. *Science*, **292**, 464–468.
8. Maxwell,P.H., Wiesener,M.S., Chang,G.W., Clifford,S.C., Vaux,E.C., Cockman,M.E., Wykoff,C.C., Pugh,C.W., Maher,E.R. and Ratcliffe,P.J. (1999) The tumour suppressor protein VHL targets hypoxia-inducible factors for oxygen-dependent proteolysis. *Nature*, **399**, 271–275.
9. Luo,W., Zhong,J., Chang,R., Hu,H., Pandey,A. and Semenza,G.L. (2010) Hsp70 and CHIP selectively mediate ubiquitination and degradation of hypoxia-inducible factor (HIF)-1α but not HIF-2α. *J. Biol. Chem.*, **285**, 3651–3663.
10. Geng,H., Liu,Q., Xue,C., David,L.L., Beer,T.M., Thomas,G.V., Dai,M.S. and Qian,D.Z. (2012) HIF1alpha protein stability is increased by acetylation at lysine 709. *J. Biol. Chem.*, **287**, 35496–35505.
11. Warfel,N.A., Dolloff,N.G., Dicker,D.T., Malysz,J. and El-Deiry,W.S. (2013) CDK1 stabilizes HIF-1alpha via direct phosphorylation of Ser668 to promote tumor growth. *Cell Cycle*, **12**, 3689–3701.
12. Lim,J.H., Lee,Y.M., Chun,Y.S., Chen,J., Kim,J.E. and Park,J.W. (2010) Sirtuin 1 modulates cellular responses to hypoxia by deacetylating hypoxia-inducible factor 1alpha. *Mol. Cell*, **38**, 864–878.
13. Seo,K.S., Park,J.H., Heo,J.Y., Jing,K., Han,J., Min,K.N., Kim,C., Koh,G.Y., Lim,K., Kang,G.Y. *et al.* (2015) SIRT2 regulates tumour hypoxia response by promoting HIF-1alpha hydroxylation. *Oncogene*, **34**, 1354–1362.
14. Liu,X., Chen,Z., Xu,C., Leng,X., Cao,H., Ouyang,G. and Xiao,W. (2015) Repression of hypoxia-inducible factor alpha signaling by Set7-mediated methylation. *Nucleic Acids Res.*, **43**, 5081–5098.
15. Kim,Y., Nam,H.J., Lee,J., Park,D.Y., Kim,C., Yu,Y.S., Kim,D., Park,S.W., Bhin,J., Hwang,D. *et al.* (2016) Methylation-dependent regulation of HIF-1alpha stability restricts retinal and tumour angiogenesis. *Nat. Commun.*, **7**, 10347.
16. Lee,J.Y., Park,J.H., Choi,H.J., Won,H.Y., Joo,H.S., Shin,D.H., Park,M.K., Han,B., Kim,K.P., Lee,T.J. *et al.* (2017) LSD1 demethylates HIF1alpha to inhibit hydroxylation and ubiquitin-mediated degradation in tumor angiogenesis. *Oncogene*, **36**, 5512–5521.
17. Shinkai,Y. and Tachibana,M. (2011) H3K9 methyltransferase G9a and the related molecule GLP. *Genes Dev.*, **25**, 781–788.
18. Wang,Y.F., Zhang,J., Su,Y., Shen,Y.Y., Jiang,D.X., Hou,Y.Y., Geng,M.Y., Ding,J. and Chen,Y. (2017) G9a regulates breast cancer growth by modulating iron homeostasis through the repression of ferroxidase hephaestin. *Nat. Commun.*, **8**, 274.
19. Ahmad,F., Dixit,D., Joshi,S.D. and Sen,E. (2016) G9a inhibition induced PKM2 regulates autophagic responses. *Int. J. Biochem. Cell Biol.*, **78**, 87–95.
20. Dong,C., Wu,Y., Yao,J., Wang,Y., Yu,Y., Rychahou,P.G., Evers,B.M. and Zhou,B.P. (2012) G9a interacts with Snail and is critical for Snail-mediated E-cadherin repression in human breast cancer. *J. Clin. Invest.*, **122**, 1469–1486.
21. Shankar,S.R., Bahirvani,A.G., Rao,V.K., Bharathy,N., Ow,J.R. and Taneja,R. (2013) G9a, a multipotent regulator of gene expression. *Epigenetics*, **8**, 16–22.
22. Lee,J.S., Kim,Y., Bhin,J., Shin,H.J., Nam,H.J., Lee,S.H., Yoon,J.B., Binda,O., Gozani,O., Hwang,D. *et al.* (2011) Hypoxia-induced methylation of a pontin chromatin remodeling factor. *Proc. Natl. Acad. Sci. U.S.A.*, **108**, 13510–13515.
23. Lee,J.S., Kim,Y., Kim,I.S., Kim,B., Choi,H.J., Lee,J.M., Shin,H.J., Kim,J.H., Kim,J.Y., Seo,S.B. *et al.* (2010) Negative regulation of hypoxic responses via induced Reptin methylation. *Mol. Cell*, **39**, 71–85.
24. Casciello,F., Al-Ejeh,F., Kelly,G., Brennan,D.J., Ngiow,S.F., Young,A., Stoll,T., Windloch,K., Hill,M.M., Smyth,M.J. *et al.* (2017) G9a drives hypoxia-mediated gene repression for breast cancer cell survival and tumorigenesis. *Proc. Natl. Acad. Sci. U.S.A.*, **114**, 7077–7082.
25. Luo,W., Hu,H., Chang,R., Zhong,J., Knabel,M., O'Meally,R., Cole,R.N., Pandey,A. and Semenza,G.L. (2011) Pyruvate kinase M2 is a PHD3-stimulated coactivator for hypoxia-inducible factor 1. *Cell*, **145**, 732–744.
26. Wu,S.Y., Lee,A.Y., Lai,H.T., Zhang,H. and Chiang,C.M. (2013) Phospho switch triggers Brd4 chromatin binding and activator recruitment for gene-specific targeting. *Mol. Cell*, **49**, 843–857.
27. Semenza,G.L., Jiang,B.H., Leung,S.W., Passantino,R., Concordet,J.P., Maire,P. and Giallongo,A. (1996) Hypoxia response elements in the aldolase A, enolase 1, and lactate dehydrogenase A gene promoters contain essential binding sites for hypoxia-inducible factor 1. *J. Biol. Chem.*, **271**, 32529–32537.
28. Jiang,B.H., Zheng,J.Z., Leung,S.W., Roe,R. and Semenza,G.L. (1997) Transactivation and inhibitory domains of hypoxia-inducible factor 1α: modulation of transcriptional activity by oxygen tension. *J. Biol. Chem.*, **272**, 19253–19260.
29. Gilkes,D.M., Xiang,L., Lee,S.J., Chaturvedi,P., Hubbi,M.E., Wirtz,D. and Semenza,G.L. (2014) Hypoxia-inducible factors mediate coordinated RhoA-ROCK1 expression and signaling in breast cancer cells. *Proc. Natl. Acad. Sci. U.S.A.*, **111**, E384–E393.
30. Cancer Genome Atlas Research, N. (2008) Comprehensive genomic characterization defines human glioblastoma genes and core pathways. *Nature*, **455**, 1061–1068.
31. Sun,L., Hui,A.M., Su,Q., Vortmeyer,A., Kotliarov,Y., Pastorino,S., Passaniti,A., Menon,J., Walling,J., Bailey,R. *et al.* (2006) Neuronal and glioma-derived stem cell factor induces angiogenesis within the brain. *Cancer Cell*, **9**, 287–300.
32. Lee,J., Kotliarova,S., Kotliarov,Y., Li,A., Su,Q., Donin,N.M., Pastorino,S., Purow,B.W., Christopher,N., Zhang,W. *et al.* (2006) Tumor stem cells derived from glioblastomas cultured in bFGF and EGF more closely mirror the phenotype and genotype of primary tumors than do serum-cultured cell lines. *Cancer Cell*, **9**, 391–403.
33. Phillips,H.S., Kharbanda,S., Chen,R., Forrest,W.F., Soriano,R.H., Wu,T.D., Misra,A., Nigro,J.M., Colman,H., Soroceanu,L. *et al.* (2006) Molecular subclasses of high-grade glioma predict prognosis, delineate a pattern of disease progression, and resemble stages in neurogenesis. *Cancer Cell*, **9**, 157–173.
34. Goswami,C.P. and Nakshatri,H. (2014) PROGgeneV2: enhancements on the existing database. *BMC Cancer*, **14**, 970.
35. Chen,Y., Zhang,B., Lei,B., Jin,L., Yang,M., Peng,Y., Kumar,A., Wang,J., Wang,C., Zou,X. *et al.* (2018) ZMYND8 acetylation mediates HIF-dependent breast cancer progression and metastasis. *J. Clin. Invest.*, **128**, 1937–1955.
36. Luo,W., Chen,I., Chen,Y., Alkam,D., Wang,Y. and Semenza,G.L. (2016) PRDX2 and PRDX4 are negative regulators of hypoxia-inducible factors under conditions of prolonged hypoxia. *Oncotarget*, **7**, 6379–6397.
37. Mahon,P.C., Hirota,K. and Semenza,G.L. (2001) FIH-1: a novel protein that interacts with HIF-1α and VHL to mediate repression of HIF-1 transcriptional activity. *Genes Dev.*, **15**, 2675–2686.
38. Wilson,A.J., Fadare,O., Beeghly-Fadiel,A., Son,D.S., Liu,Q., Zhao,S., Saskowski,J., Uddin,M.J., Daniel,C., Crews,B. *et al.* (2015) Aberrant over-expression of COX-1 intersects multiple pro-tumorigenic pathways in high-grade serous ovarian cancer. *Oncotarget*, **6**, 21353–21368.
39. Kuang,X.L., Zhao,X.M., Xu,H.F., Shi,Y.Y., Deng,J.B. and Sun,G.T. (2010) Spatio-temporal expression of a novel neuron-derived

neurotrophic factor (NDNF) in mouse brains during development. *BMC Neurosci.*, **11**, 137.
40. Perez-Perri,J.I., Dengler,V.L., Audetat,K.A., Pandey,A., Bonner,E.A., Urh,M., Mendez,J., Daniels,D.L., Wappner,P., Galbraith,M.D. *et al.* (2016) The TIP60 complex is a conserved coactivator of HIF1A. *Cell Rep.*, **16**, 37–47.
41. Ueda,J., Ho,J.C., Lee,K.L., Kitajima,S., Yang,H., Sun,W., Fukuhara,N., Zaiden,N., Chan,S.L., Tachibana,M. *et al.* (2014) The hypoxia-inducible epigenetic regulators Jmjd1a and G9a provide a mechanistic link between angiogenesis and tumor growth. *Mol. Cell. Biol.*, **34**, 3702–3720.
42. Chen,H., Yan,Y., Davidson,T.L., Shinkai,Y. and Costa,M. (2006) Hypoxic stress induces dimethylated histone H3 lysine 9 through histone methyltransferase G9a in mammalian cells. *Cancer Res.*, **66**, 9009–9016.
43. Casciello,F., Windloch,K., Gannon,F. and Lee,J.S. (2015) Functional role of G9a histone methyltransferase in cancer. *Front. Immunol.*, **6**, 487.